

Scanning and Transmission Electron Microscopy of Human Prostatic Acinar Cells

Marie P. Stone¹, Kenneth R. Stone¹, Peter Ingram², Don D. Mickey,¹
and David F. Paulson¹

¹Department of Surgery, Division of Urology, Duke University Medical Center, and

²Chemistry and Life Science Division, Research Triangle Institute, Research Triangle Park, Durham, North Carolina, USA

Received: November 17, 1976

Summary. Benign hyperplastic and neoplastic human prostate tissue samples were obtained by needle biopsy, transurethral resection or open prostatectomy. Acinar cells of both types of tissues were examined in the scanning electron microscope. It had been reported previously that adenocarcinoma acinar cells were more heterogeneous in size and shape than BPH acinar cells; the purpose of this study was to determine if there were surface morphology differences between the two types of tissues. Acinar cells were found to be extremely heterogeneous in their surface morphologies; three major types of surface morphologies were present - microvillous, ruffled, and bare. Within each class of surface morphology there was heterogeneity, both in the size and density, of surface structures present. Microvillous, ruffled, and bare cells appeared to be present in normal, BPH, and neoplastic acini with no significant qualitative or quantitative differences in surface morphologies. Infrequently, it was possible to distinguish between well-differentiated and poorly-differentiated carcinomas because cells of the latter tissues were present in sheets rather than acini and appeared flat and totally devoid of surface detail. The SEM studies also sought to determine a marker to establish the origin of prostate tissue culture cells as normal, BPH or cancerous. Surface morphologies from tissues could be traced into the tissue cultures; again, three types of cells are present - bare, microvillous, and ruffled. However, since surface morphology does not appear to be a distinguishing feature of the pathology of the tissue it cannot provide a distinguishing marker for the origin of tissue culture cells.

Scanning electron microscopy also provided an opportunity to observe possible secretory mechanisms and products in the prostate acinar cells.

Key words: Benign prostatic hyperplasia - Prostatic adenocarcinoma - Scanning electron microscopy - Transmission electron microscopy.

The ultrastructure of acinar cells from normal prostate, benign prostatic hyperplasia (BPH), and prostatic adenocarcinoma has been investigated in several transmission electron microscopy (TEM) studies (3, 4, 9, 10, 19, 20). Tall cuboidal cells with nuclei situated in the basal portion line the normal acinus. Secretory granules are evident at the apical

pole and in the supranuclear region. These characteristics, as well as the position and number of other cell organelles, are generally similar for acinar cells of normal and benign hyperplastic tissues (4, 9, 20) though some studies indicate there may be intercellular spaces, or lacunae, in the BPH acini (4). Well-differentiated carcinoma cells present similar

ultrastructure, though close observation indicates a greater variability in number and size of cell organelles (4, 9, 19, 35).

Preliminary scanning electron microscopy (SEM) studies examined the surface morphology of human prostatic acinar cells (7, 8, 35). Clark et al. indicated that surface differences might exist in acinar cells of normal and BPH tissues (7, 8). Stone et al. could find no detectable differences in the surface morphologies of normal (unpublished observation), BPH, and well-differentiated carcinoma acinar cells. The acinar cells of the neoplastic prostate are consistently more heterogeneous in size and shape than acinar cells of BPH and control tissues; yet normal, BPH, and carcinoma acinar cells have the same types of surface structures (35). The present study utilizes both scanning and transmission electron microscopy to correlate surface morphology of prostate acinar cells with ultrastructure to determine if surface morphology provides a marker for the classification of a cell as normal, BPH, or cancerous and to determine if the surface morphology of acinar cells in tissue can be used as a marker to identify acinar cells in vitro.

MATERIALS AND METHODS

Source and Fixation of Tissue

Prostatic tissue was obtained by needle biopsy, transurethral resection, or open prostatectomy from patients with BPH or adenocarcinoma. The tissues, which were placed in cold medium in the operating room, were divided into several portions. One was for tissue culture while another was fixed in 5% glutaraldehyde in 0.1 M sodium cacodylate buffer (pH 7.4) at room temperature for 1 hour and stored at 4°C for 24 hours. Samples were fixed immediately following excision from the patient, or within 1 hour of surgery. After fixation, the tissues were cut into slices approximately 1 mm thick.

Determination of Tissue Pathology

In order to determine the pathology of a specific acinus, several parameters were used. The pathology report of the excised tissue was reviewed. It was noted whether discrete foci, or general areas of the tissue, were involved in adenocarcinoma of prostate; the stage of the adenocarcinoma was also recorded from the pathology report. However, the most important criteria for determining the pathological state of a specific acinus

were (1) shape, (2) size, and (3) the ordered arrangement of the cells in relation to each other, the stroma, and surrounding acini when examined at low magnification (60X) in the scanning electron microscope. The BPH acini were easily recognizable by these criteria. Differentiation between the normal and well-differentiated adenocarcinoma acini was more difficult. Twenty-four (24) BPH tissue samples and 21 adenocarcinoma samples (well-differentiated to poorly-differentiated as determined by the original pathology reports) were examined in this study.

Scanning Electron Microscopy

After fixation in glutaraldehyde the tissue slices were rinsed in 0.1 M sodium cacodylate buffer (pH 7.4) containing 5% sucrose and postfixed for 1 hour in 1% osmium tetroxide in sodium cacodylate buffer (pH 7.4). SEM specimens were rinsed in 0.1 M sodium cacodylate buffer (pH 7.4) and processed for scanning electron microscopy as described in detail elsewhere (35). The tissues were dehydrated by washing in a graded series of ethanol and subjected to critical point drying (Denton Vacuum Critical Point Dryer) using Freon 113 as the intermediate fluid and liquid carbon dioxide as the transitional fluid. The dried specimens were mounted on scanning electron microscope stubs, coated with platinum and carbon in a JEOL vacuum evaporator equipped with a rotary tilting stage and examined in an Etec "Autoscan" scanning electron microscope operated at 10 or 20 KV.

Transmission Electron Microscopy

After fixation in 5% glutaraldehyde TEM tissue specimens were washed and postfixed in osmium tetroxide as described above for SEM specimens. TEM specimens were dehydrated in a graded series of ethanol and embedded in epoxy resin (18). Sections for light microscopy were cut at 0.5 μ thickness on a Porter-Blum ultramicrotome and stained with toluidine blue (6, 27, 33). Thin sections for TEM were stained with 1% uranyl acetate (38), and Sato's lead stain (29). All TEM specimens were examined and photographed in a Philips 300 electron microscope. TEM specimens were prepared as a control to determine if the samples processed for SEM and subsequently processed for TEM were substantially changed because of the double processing.

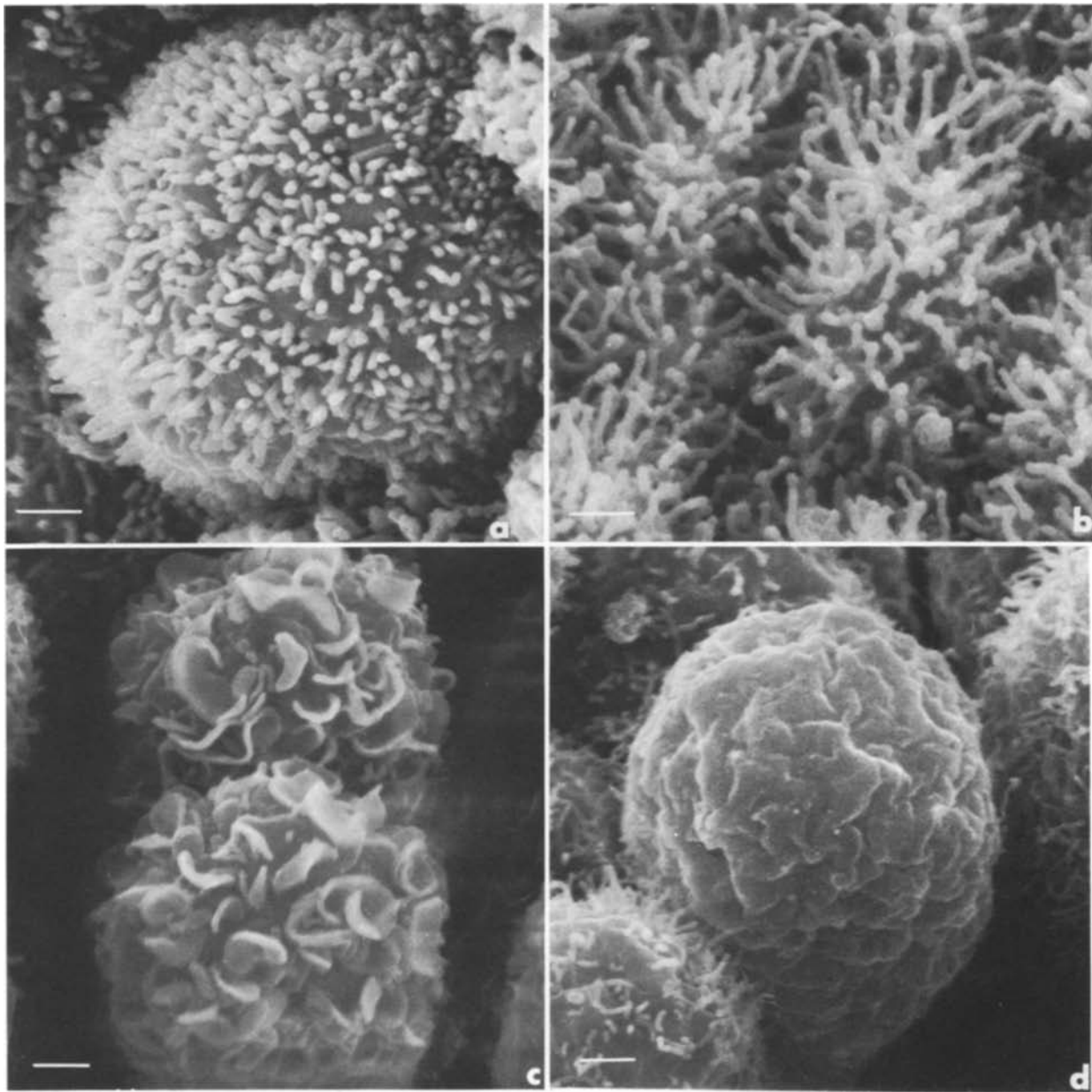


Fig. 1. Scanning electron micrographs illustrating the variation in cell surface morphologies present in prostate acinar cells. a) Cell from a BPH acinus with microvillous surface structure. The microvilli are uniform and $0.4\text{--}0.5\mu$ in length. b) Cells from a BPH acinus with extremely long microvilli ($1\text{ to }1.5\mu$). c) Cells from an acinus in well-differentiated adenocarcinoma tissue with ruffle surface structure. Ruffles are relatively uniform in size ($0.5\text{--}2.0\mu$ length, $0.4\text{--}0.5\mu$ height, 0.15μ diameter). d) A cell from an acinus in well-differentiated adenocarcinoma tissue with a bare but undulating apical surface. Bars equal 1μ

Scanning Electron Microscopy Specimens Prepared for Transmission Electron Microscopy

Scanning stereomicrographs were used when viewing the SEM specimens in a dissecting microscope to identify acini which had been scanned and were selected for subsequent TEM studies. Selected acini were processed through propylene oxide and embedded in Epon (18) in flat embedding molds under a dissecting microscope in order to maintain the specific orientation desired for sectioning.

Tissue Culture

Prostatic glandular explants isolated as described elsewhere (34) were seeded into petri dishes containing collagen-coated glass coverslips (14). Five days later the prostatic tissue culture cells were rinsed in fresh medium and fixed at room temperature for 30 minutes in a 1:1 mixture of 4% glutaraldehyde and fresh medium (39). The cultures were placed in 4% glutaraldehyde at 4° for 24 hours and rinsed in 0.1 M sodium cacodylate buffer (pH 7.4). Coverslips were dehydrated

through a graded series of ethanol and processed for scanning electron microscopy as described for prostatic tissue specimens except that Freon 13, instead of liquid CO₂, was used as the transitional fluid in a Bomar SPC-900 Ex Critical Point Dryer.

RESULTS

Scanning Electron Microscopy

Acinar cells of normal, BPH, and cancerous prostate tissues when examined in the scanning electron microscope exhibit great variation in surface morphology. The cell surface morphologies were classified as microvillous, ruffled, or bare (Figs. 1a-d).

Microvillous Cells. Cells with microvilli of many sizes and varying density are the most numerous surface morphology class of normal, BPH, and well-differentiated carcinoma cells (Figs. 1a, 1b, 2a-d, 10a-e). Short, stubby microvilli (0.1-0.2 μ length, 0.05-0.1 μ diameter) are present on some villous cells as indicated previously (35) ranging from relatively few microvilli per cell (Fig. 2a) to extremely dense populations of microvilli (Fig. 2d). Heterogeneity in the length of microvilli as well as in numbers of microvilli per cell is also noted. Figure 1a represents an intermediate microvillous length (0.4-0.5 μ) and Figure 1b represents the longest class of microvilli seen on the prostate acinar cell surface (1-1.3 μ). Figure 2d represents another interesting variation in microvillar structure; the microvilli are extremely numerous and appear clumped.

Ruffled Cells. Surface structures are found on acinar cells which, at the extreme end of the spectrum, qualify for the term ruffles as in Figure 1c (0.5-2 μ length, 0.4-0.5 μ height, 0.15 μ thickness). In Figure 2b ruffles are identified on cell surfaces (indicated by arrows); however it is difficult in other areas of the same acinus to identify certain structures as "ruffles" or as collapsed microvilli (as in Fig. 2a). The structures indicated in Figure 2a by double arrows are ruffles as shown by stereo micrographs. In agreement with recent literature (1) these structures (in Fig. 2a) are designated as ridge-like (0.3-0.9 μ length, 0.1-0.2 μ height), or microplacae, rather than ruffles. The numbers of ruffles and microplacae per cell vary greatly.

Bare Cells. The bare cells are divided into two general types - cells which appear balloon-like, with no microprojections and cells which appear identical to microvillous

and ruffled cells in shape, but have an undulating surface rather than microplacae or microvilli (Fig. 1d).

In general, the microvillous cells comprise 90% or more of the acinar cells surfaces scanned. The cell surface extremes such as the long microvillous cell (Fig. 1b), the ruffled cell (Fig. 1c), and the bare cell, comprise less than 10% of the cell population. Ruffled cells are found in groups in an acinus, as are the cells with long microvilli. Acinar cells with varying surface morphologies appear in adjacent areas of the same acinus (Figs. 2a-d) and all three types of surface morphologies (microvilli, ruffles, and bare) are observed in all three types of prostate tissues - normal, BPH, and adenocarcinoma.

Tissue Culture. Primary tissue cultures of glandular explants of BPH and adenocarcinoma prostate tissues were examined with the scanning electron microscope. The results are illustrated in Figure 3a-d. Cells spreading out onto the surface of the petri dish display the same classes of surface morphology found in the prostate acini. There are four classes, flat epithelial-like cells essentially devoid of surface structure, cells with numerous short (0.1-0.2 μ) microvilli, tissue culture cells with much longer (0.9 μ) microvilli (or both long and short microvilli), and tissue culture cells with ridge-like membranous structures. The surface morphologies of tissue culture cells are representative of those found in tissue, both in classification and percentages of the total population found in each class, with microvillous cells present in the greatest number. The long microvillous cells as well as the ruffled cells appear in groups in the tissue culture monolayer, as they do in the prostatic acini.

Transmission Electron Microscopy Studies of Acini Examined by SEM

Figure 4 is a representative section through the same acinus from which Figure 2a and 2b were photographed. Cell a probably corresponds closely to scanning electron micrograph Figure 1c, cell b corresponds to Figure 1a and cells d and e, to Figure 1d.

The apex of cell a has extensions (0.7-1.6 μ length) into the lumen of the gland. Between the extensions there is granular material which is probably a secretory product. There is also a large vesicle at the surface of cell a, which is filled with a similar granular secretory substance. The remainder of the apex of the cell is filled with electron

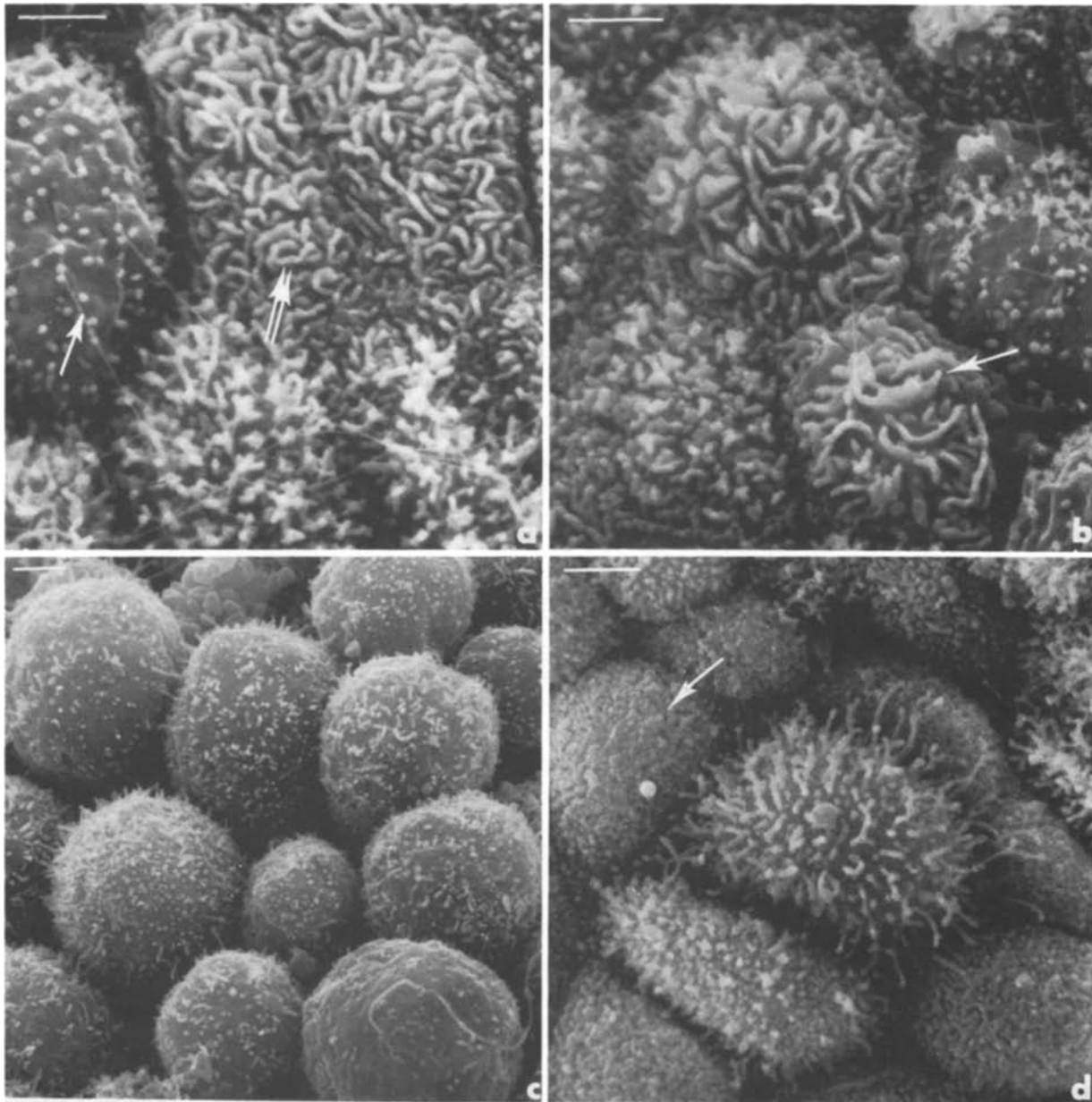


Fig. 2. Scanning electron micrographs of cells in a BPH acinus illustrating several classes of surface structure within a single tissue specimen. a) A cell with sparse, stubby microvilli ($0.1-0.2\mu$ length, $0.05-0.1\mu$ diameter) is indicated by the single arrow. Two cells in the center of the micrograph exhibit structures which are microplicae (indicated by double arrows). The cells at the bottom of the micrograph are covered with long microvilli. b) Cells adjacent to acinar cells in micrograph 2a. Definite ruffled surface structure present on two center cells is indicated by the arrow. A cell with sparse, stubby microvilli is present, as are two cells with a mixture of microvillous and ruffle surface structure. c) Cells exhibit sparse, short microvilli, or a mixture of both long and short microvilli. d) The arrow indicates a cell with numerous, clumped microvilli. Two cells in the center of the micrograph exhibit long microvilli. Bars equal 2μ

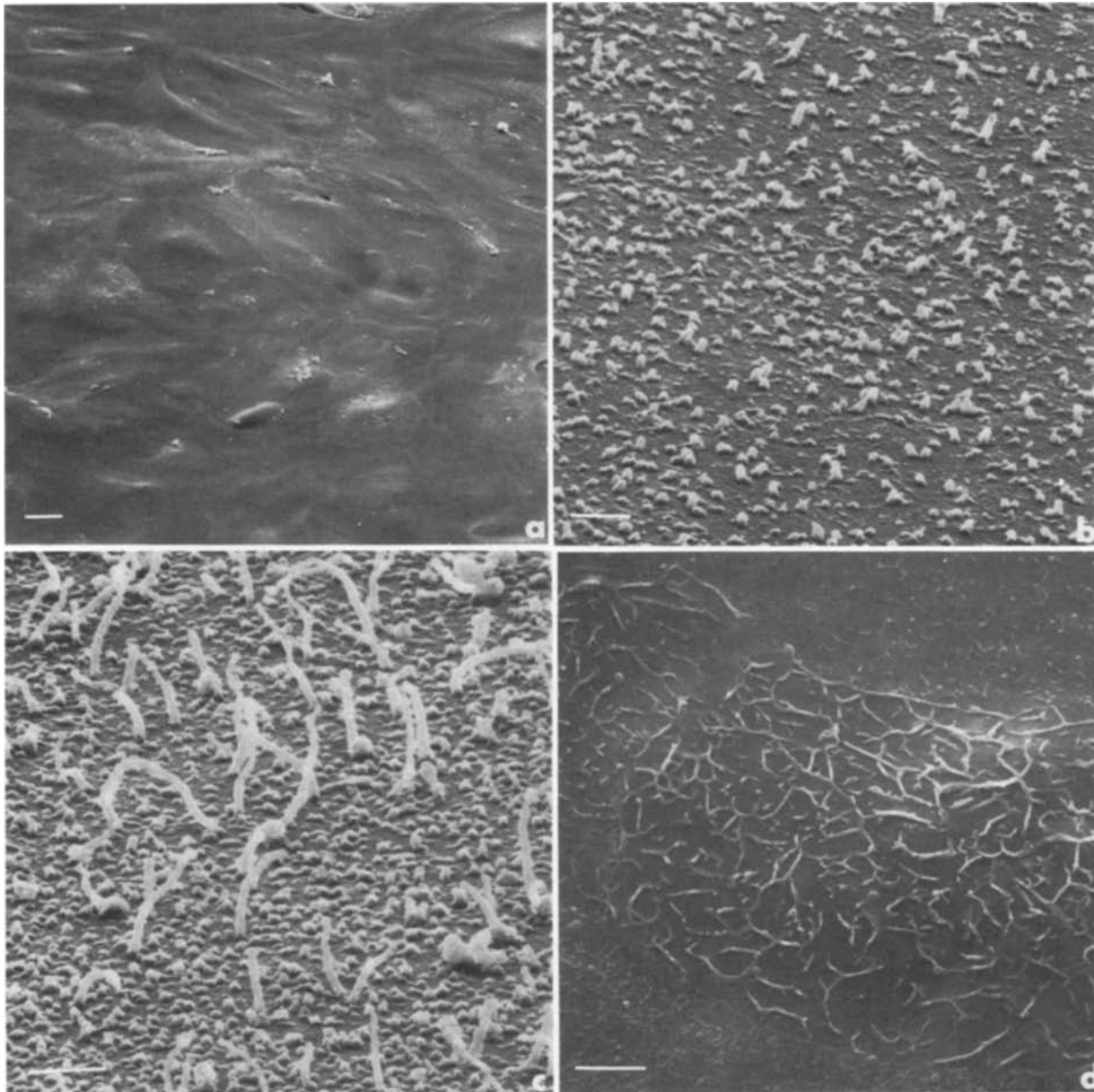


Fig. 3. Scanning electron micrographs of acinar cells in vitro: a) in the form of a monolayer (Bar equals 25μ), b) tissue culture cells with the same types of surface morphologies described for tissue acinar cells - microvilli (Bar equals 1μ), c) long microvilli (Bar equals 1μ), d) microplicae (Bar equals 5μ)

dense secretory granules. The apical membrane of cell b has numerous microvillous extensions (0.5μ length, $0.07-0.1\mu$ diameter); the cell contains electron-dense secretory granules and several large vacuoles filled with granular material. Cell c appears to have fewer and shorter microvilli ($0.1-0.15\mu$) than cell b; secretory granules or vacuoles are not evident. Cell d has a bare but undulating surface; large vacuoles, some

filled with granular substances, are most numerous in the apical portion of the cell though a few electron-dense secretory granules are present. Cell e, which is also bare of surface structure, contains electron-dense secretory granules and large vacuoles.

Figure 5 is a section from an area of the acinus in Figure 2c, and the cells correspond in surface structure to Figure 1d. There are a few undulations in the apical membranes

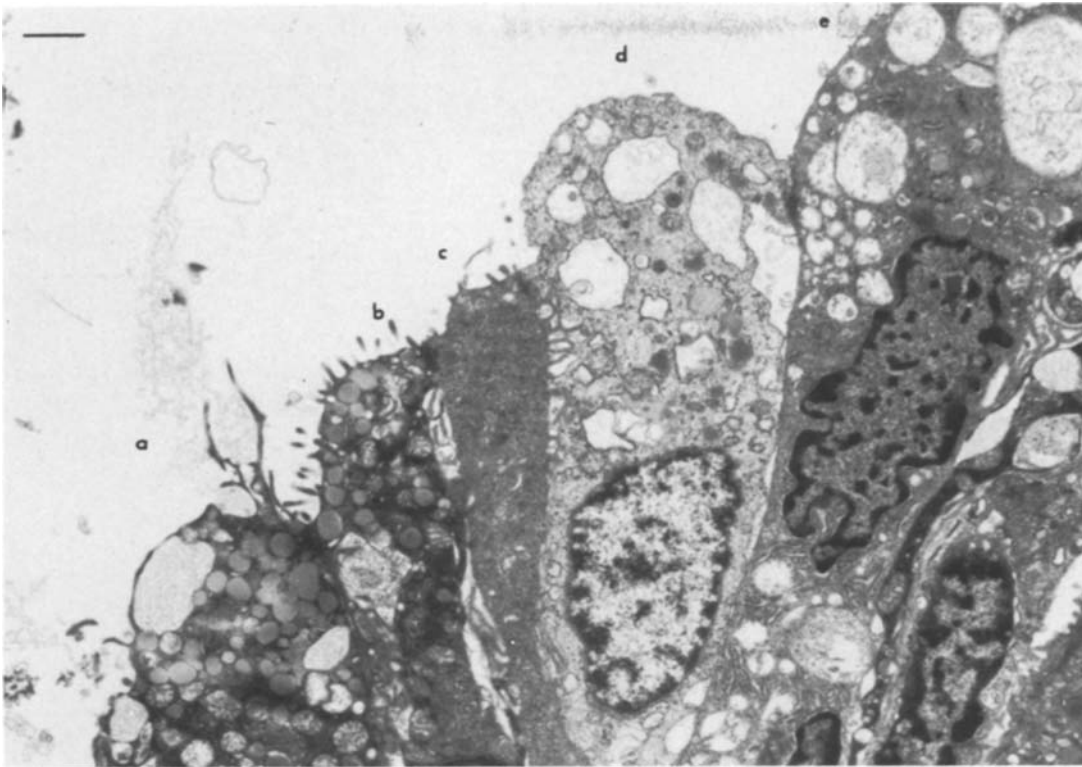


Fig. 4. Transmission electron micrograph of a section through the same BPH acinus that was examined by SEM in Figures 2a and 2b. Five cells are present which are labeled a-e, and which exhibit microvillous (b, e) ruffled (a) and bare but undulating apical surfaces (d, e). Bar equals 1 μ

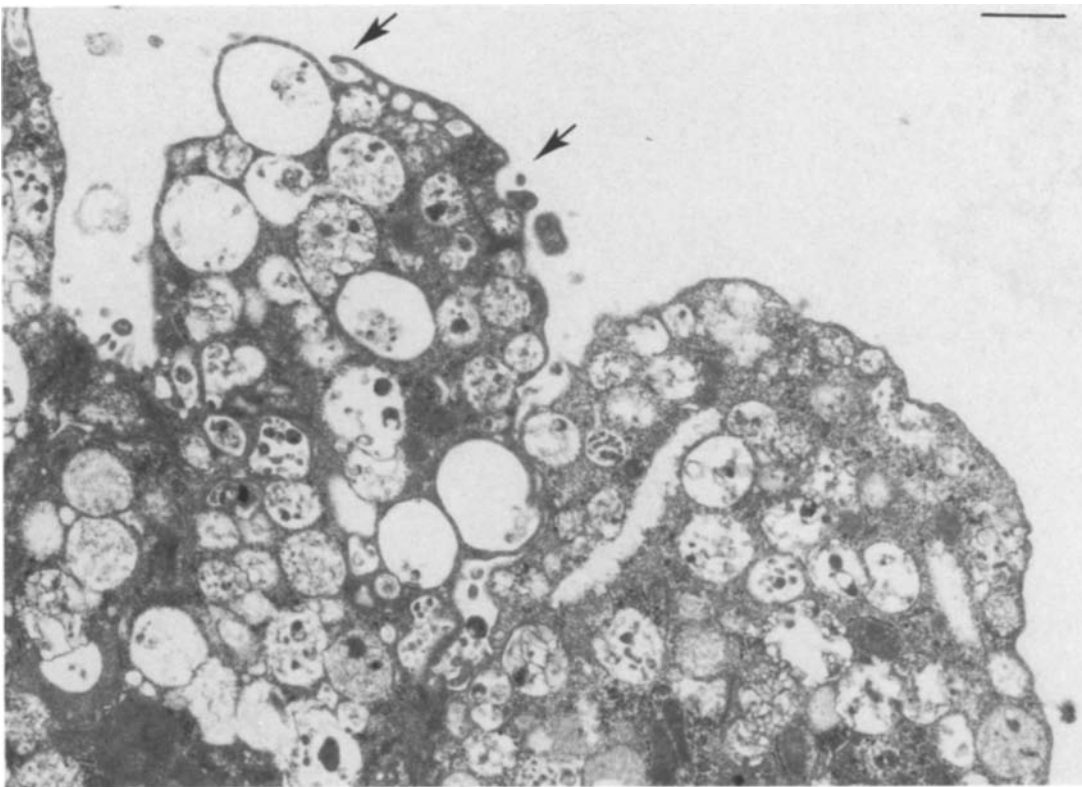


Fig. 5. Transmission electron micrograph of a section of an acinus in the BPH tissue scanned in Figures 2a-d. Two cells exhibit rather bare but undulating surface membranes. Secretion products in the process of extrusion into the lumen are indicated by arrows. Bar equals 1 μ

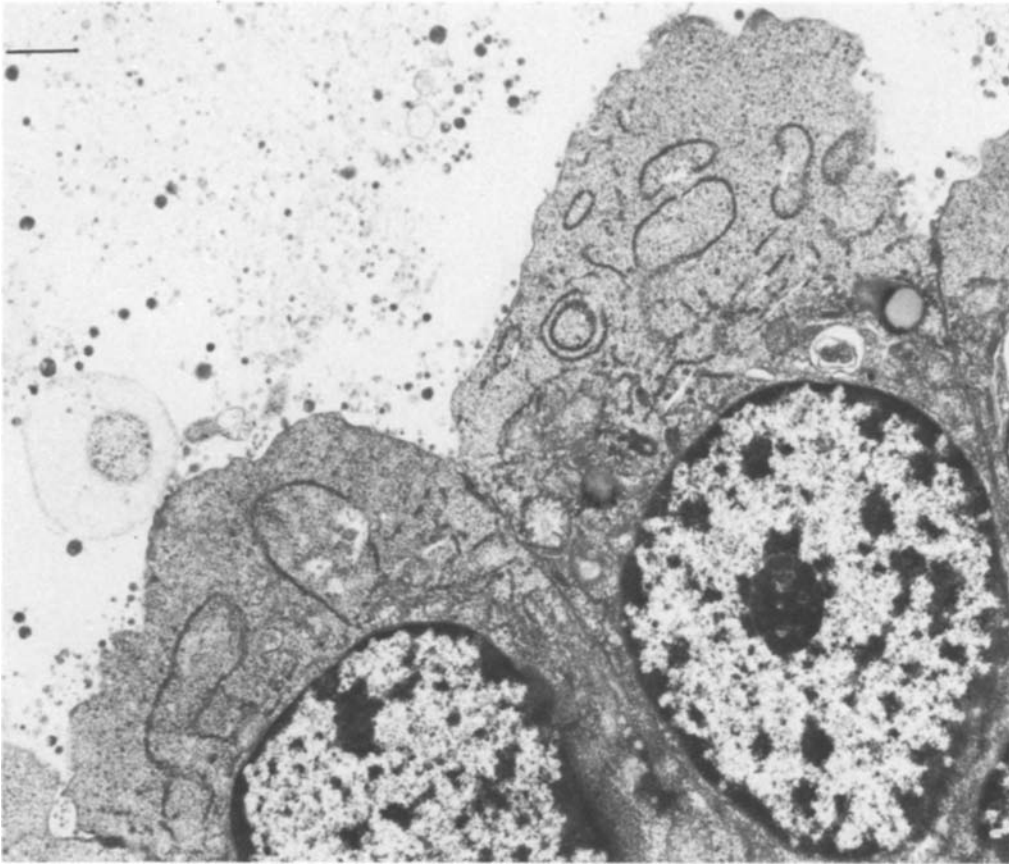


Fig. 6. Transmission electron micrograph of a section from the acinus scanned in Figure 2c. The cells have a bare but undulating membrane. Few secretory vacuoles, or granules, are present so that other cell organelles are evident. Bar equals 1μ

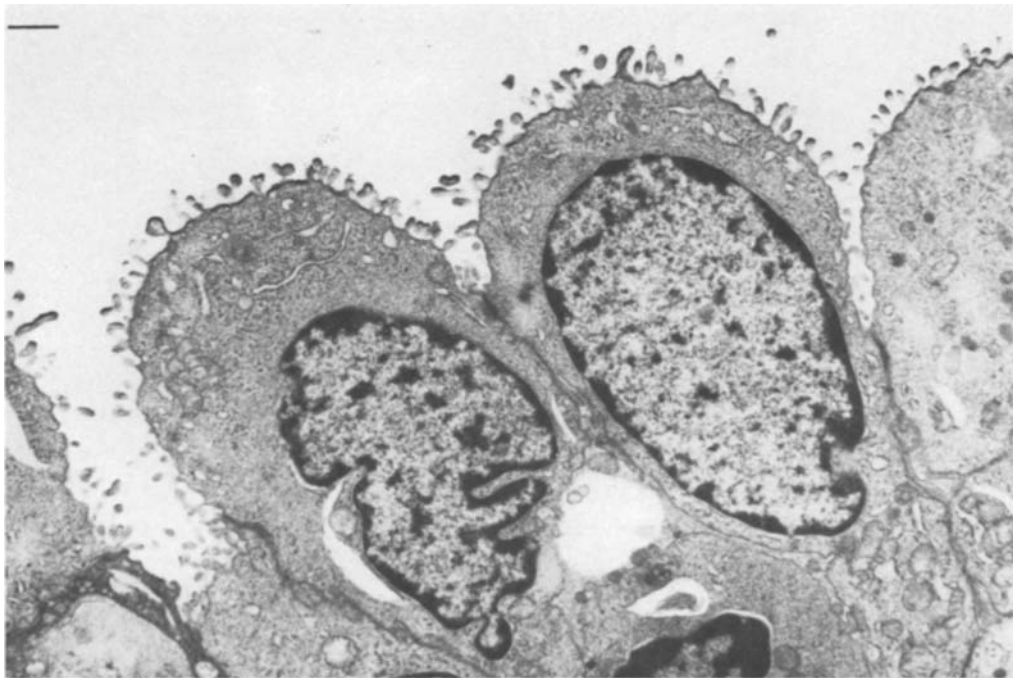


Fig. 7. Transmission electron micrograph of a section of the acinus scanned in Figure 2d. Short clumped microvilli are present on the apical surface of the cells, the platinum-carbon coating for SEM is also evident on the surface of the cells. No secretory vacuoles or granules are evident. Bar equals 1μ

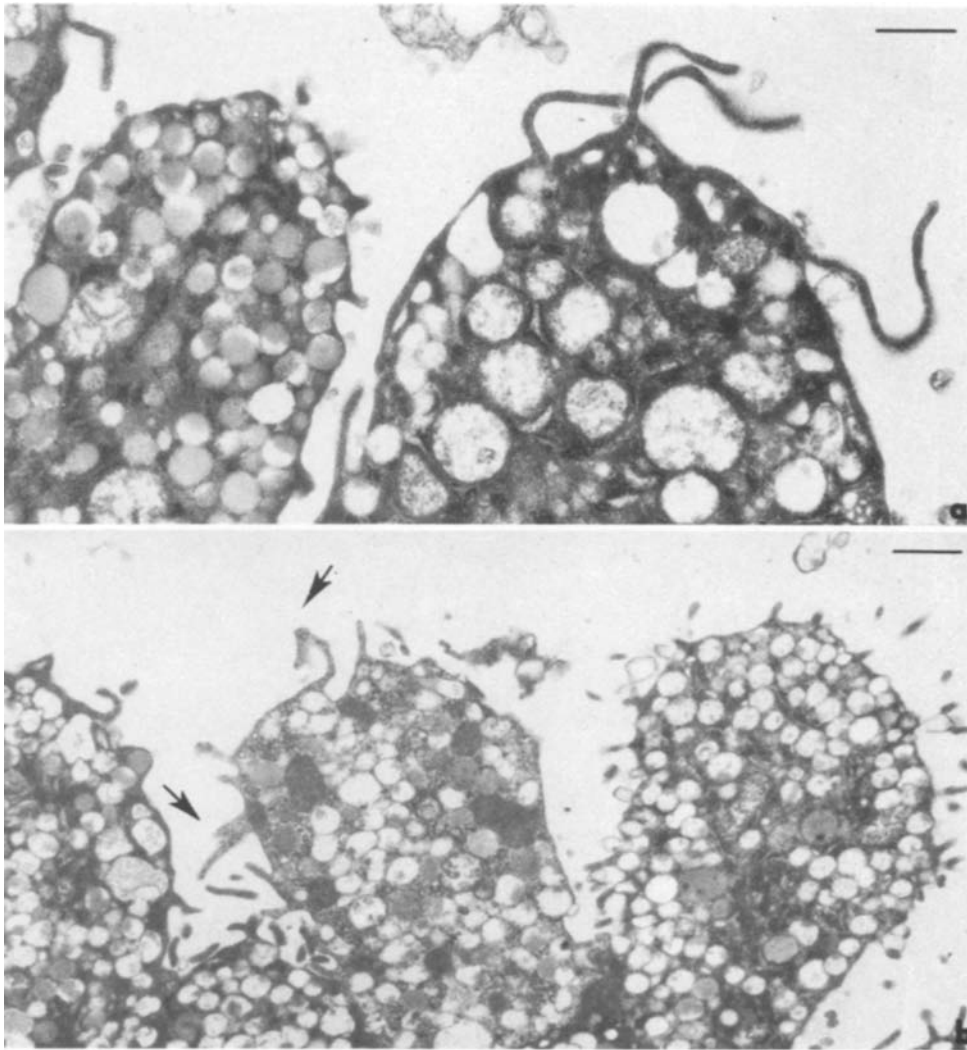
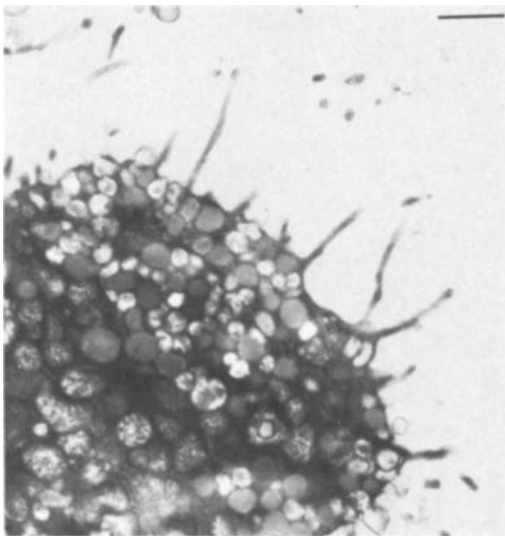


Fig. 8. Transmission electron micrographs of the BPH acinus in Figures 2a and b. a) Long projections on surface of cell probably represent ruffles. b) Structure indicated by arrows are also ruffles. Bar equals 1μ



and numerous secretory vacuoles are present. A few mitochondria are present but other cell organelles are not evident in this section.

Figure 6 is a representative section of the acinus in Figure 2c though sectioned through a slightly different area as evidenced by the granular secretions present in the lumen. Granular secretion would give the cells in this section the appearance of Figure 10b when viewed in the scanning electron microscope. The apical membrane surfaces are bare but undulating. Convolved cisternae of rough

Fig. 9. Transmission electron micrograph of a cell from the BPH acinus in Figure 2d. Microvilli are 1 to 1.5μ length; this cell is probably similar in surface structure to the cell in the center of Figure 2d. Bar equals 1μ

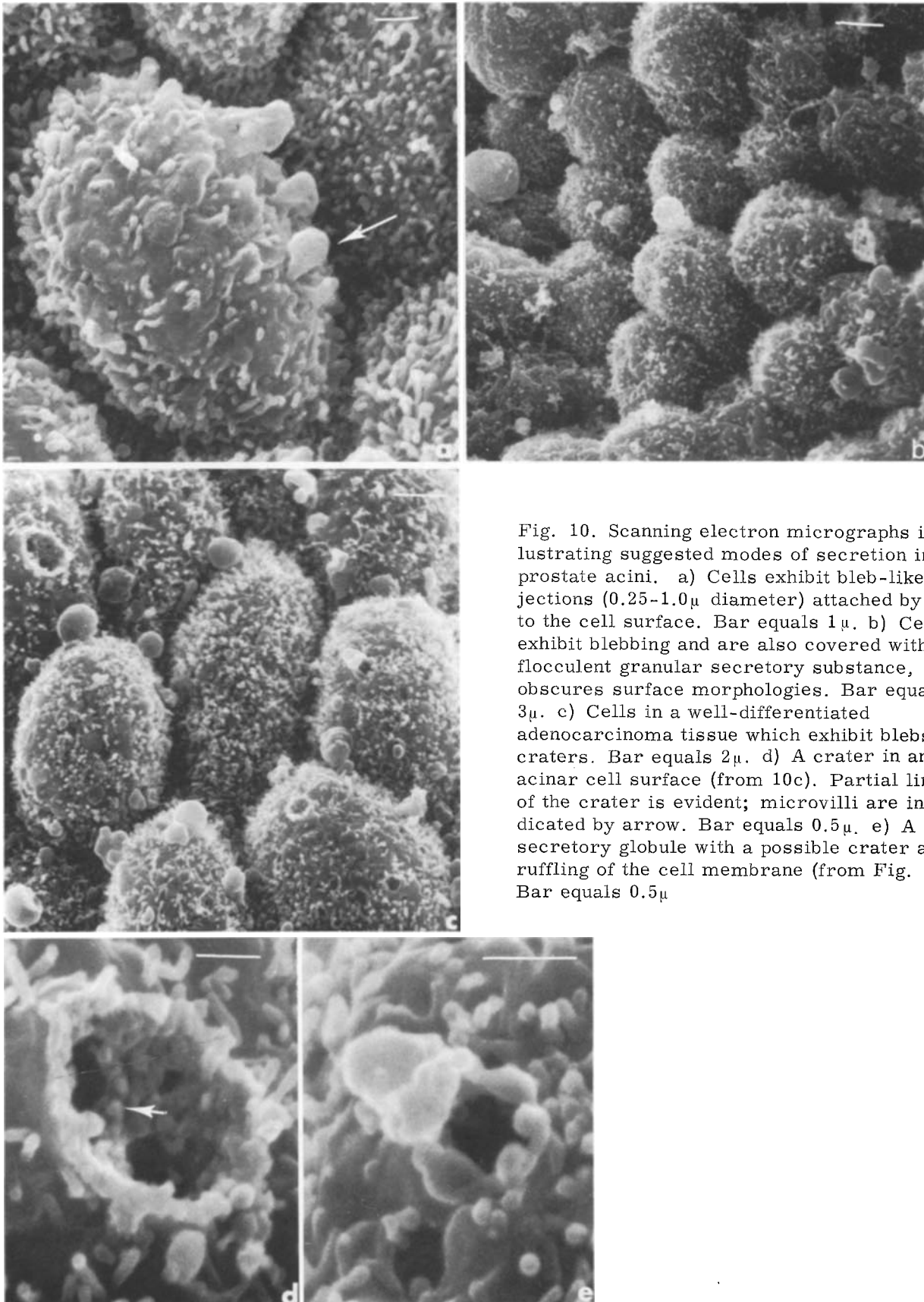


Fig. 10. Scanning electron micrographs illustrating suggested modes of secretion in prostate acini. a) Cells exhibit bleb-like projections ($0.25\text{--}1.0\mu$ diameter) attached by stalks to the cell surface. Bar equals 1μ . b) Cells exhibit blebbing and are also covered with a flocculent granular secretory substance, which obscures surface morphologies. Bar equals 3μ . c) Cells in a well-differentiated adenocarcinoma tissue which exhibit blebs and craters. Bar equals 2μ . d) A crater in an acinar cell surface (from 10c). Partial lining of the crater is evident; microvilli are indicated by arrow. Bar equals 0.5μ . e) A secretory globule with a possible crater and ruffling of the cell membrane (from Fig. 10c). Bar equals 0.5μ .

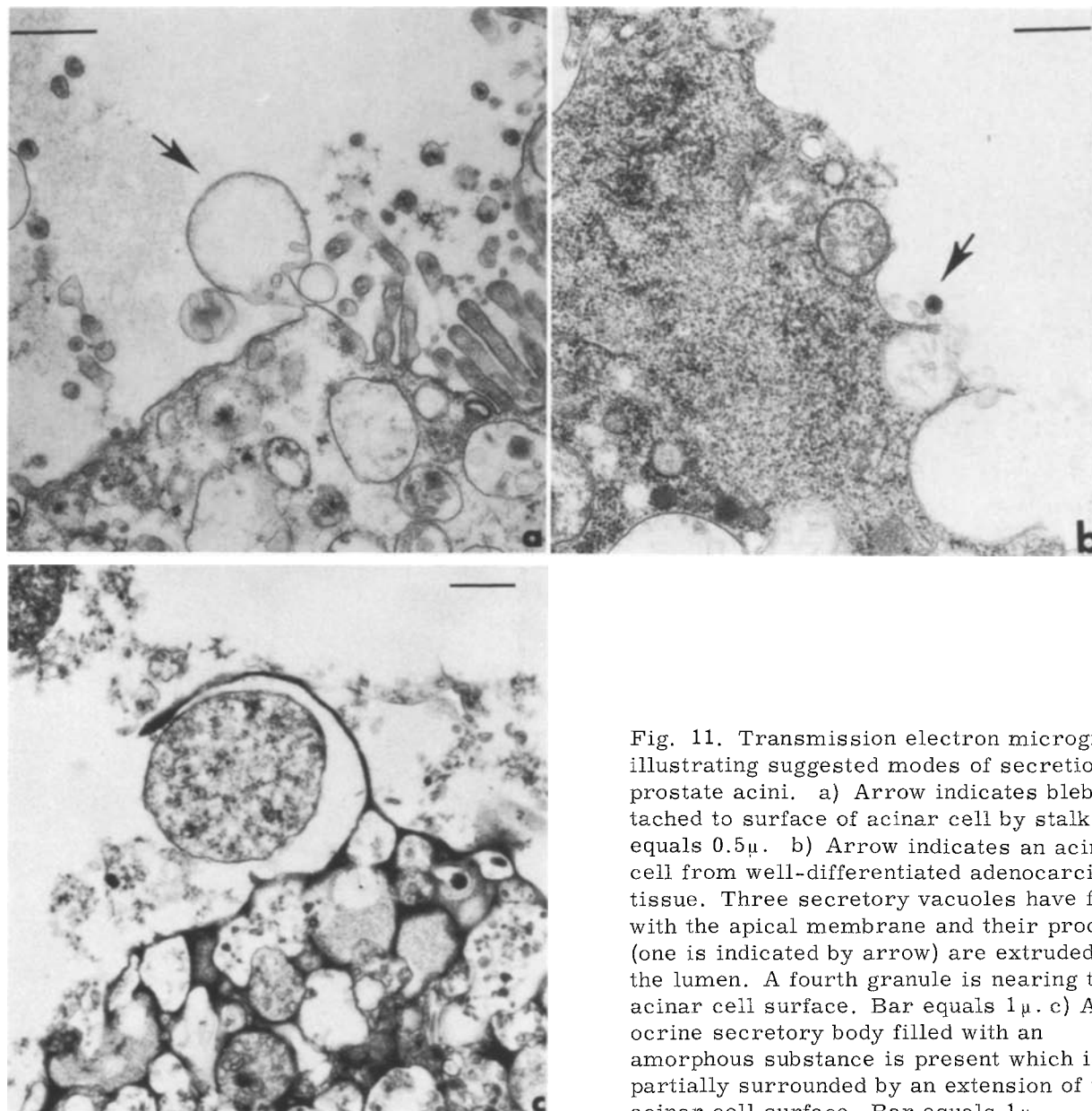


Fig. 11. Transmission electron micrographs illustrating suggested modes of secretion in prostate acini. a) Arrow indicates bleb attached to surface of acinar cell by stalk. Bar equals 0.5μ . b) Arrow indicates an acinar cell from well-differentiated adenocarcinoma tissue. Three secretory vacuoles have fused with the apical membrane and their products (one is indicated by arrow) are extruded into the lumen. A fourth granule is nearing the acinar cell surface. Bar equals 1μ . c) An apocrine secretory body filled with an amorphous substance is present which is partially surrounded by an extension of the acinar cell surface. Bar equals 1μ .

endoplasmic reticulum are present in both cells. Numerous mitochondria are present in the perinuclear region though perhaps not as well preserved as those acini prepared directly for TEM. The Golgi apparatus and secretory vesicles are difficult to identify though three structures are present which appear to be lipid bodies. The nuclei are situated in the basal region and prominent nucleoli are present. Junctional complexes are evident near the luminal surfaces of the cells.

Figure 7 is a section of the acinus shown in Figure 2d. Most of the cells exhibit the clumped microvilli evident in the scanning

electron micrograph. Very few cellular organelles are present; though some rough endoplasmic reticulum and several mitochondria can be distinguished. Few secretory granules or vesicles are present.

Figures 8a and b are representative of other sections of the acinus shown in Figures 2a and b. One cell in Figure 8a contains electron-dense secretory granules and has short stubby apical projections (0.15μ diameter, 0.15 – 0.3μ length). The second cell in Figure 8a also contains secretory granules; and the apical membrane has several extremely long extensions (2.5μ). The cells in Figure 8b contain many secretory vesicles, both

electron-dense and filled with granular material. Structures which appear to be ruffles (0.3-0.6 μ height) are indicated by arrows. The second cell in Figure 8a would correspond to Figure 1c; the surface structure of the center cell in Figure 8b also corresponds to that of the cells in Figure 1c.

Figure 9 is a section of the acinus in Figures 2a and b showing a single cell and its surface projections. The length, (1.2 μ) of the microvilli classify it as an acinar cell with long microvilli (such as Figs. 1b and 2d). This cell contains numerous electron-dense secretory granules as well as secretory vacuoles.

The three types of acinar cell surface morphologies which are present when prostate tissues are examined in the scanning electron microscope are also present in transmission electron micrographs of the same acinus. Figures 5 and 6 are representative of the bare cells; Figures 8a and b, of the ruffled cells; and Figures 7 and 9, of the microvillous cells.

Secretion

Prostate acinar cells are secretory cells and the scanning electron microscope has presented an opportunity to study the possible secretory mechanisms and products of acinar cells. The apical portion of the acinar cell in Figure 10a has several bleb-like projections attached to its surface by stalks. These projections may correspond to apocrine secretion. Scanning electron micrographs 10b-e can be interpreted in a similar manner. Blebs of varying sizes (0.4-1.4 μ diameter) are present on the apical surfaces of the cells; similar globules also appear free in the acinar lumen. Only the blebs and free globules are generally seen; though, in less than 0.5% of the acinar cell population craters in the cell surface may occur in the same areas as the blebbing. The craters have a demonstrable lining (Figs. 10d and 10e); in Figure 10d microvilli can be identified in the crater. It is possible that craters may also be a part of the secretory process of prostate cells. The most frequently seen secretory product is the flocculent granular material in 10b which obscures the acinar cell surface structure.

The transmission electron micrographs in Figures 11a-c can be correlated with the scanning electron micrographs of Figures 10a-e. In Figure 11a, three membranous blebs (0.2-0.7 μ diameter) are adjacent to the apical cell membrane; the largest bleb is attached by a stalk-like projection to the apical cell membrane. These blebs are the same size range as those in Figure 10a (0.2-0.8 μ dia-

meter). The membranes of four secretory vacuoles have fused with the apical cell membrane in Figure 11b and are in the process of emptying their products into the lumen of the acinus. In Figure 11c the apical portion of the cell is filled with secretory vacuoles. There is a ruffle of the cell membrane and within the area enclosed by the ruffle is a membrane enclosed amorphous secretory body. Transmission electron micrograph 11c appears to be analogous to scanning electron micrograph 10e. The transmission electron micrograph in Figure 5 may be illustrative of the situation shown in Figure 10c. Several secretory vacuoles have combined with the cell membrane and their contents appear extruded into the acinar lumen. One secretory vacuole at the apex of the cell (0.7 μ diameter) and another on the right side of the apical membrane (0.6 μ diameter) have created blebs in the cell's apical surface.

DISCUSSION

Recent studies of several human tissues have sought to determine if there are differences among the surface morphologies of normal, benign, and neoplastic tissue which can be defined by SEM (7, 8, 12, 24, 28, 31, 32, 35).

In a previous publication Stone et al. stated that "though areas of heterogeneous acinar cells can be seen in BPH tissues, the acinar cells of the neoplastic prostate are consistently more heterogeneous in size and shape than the acinar cells of benign hyperplastic tissues". There are certain restrictions which must be considered in such a statement; one restriction involves the stage of differentiation of the neoplastic cell. Moderate- to poorly-differentiated carcinomas show much heterogeneity in acinar cell size and shape but a well-differentiated adenocarcinoma does not. It is impossible to differentiate between a normal, BPH, or well-differentiated carcinoma cell on the basis of its size or shape.

The heterogeneity in size and shape of carcinoma cells in the prostate parallels the observation by Spring-Mills that carcinoma cells in mammary ducts show a greater variation in size and shape than mammary duct cells in "normal" areas (32). Siew has observed that carcinoma cells of the colon vary in size and shape compared to the uniform size, shape, and polarity of normal colon cells (31). Both the Spring-Mills and Siew studies indicate that differences in surface morphology (i. e. pleomorphic microvilli) may provide another distinguishing factor between "normal" and cancerous areas; Polliack has

also suggested, in a study of leukaemic cells, that surface morphologies may provide a useful adjunct in the study and eventual diagnosis of leukaemia. In certain leukaemias the microprojections, such as microvilli and ruffles, of leukaemic cells are better developed and larger than those of normal cells (24).

Though several classes of surface morphologies exist in prostatic carcinoma cells, they do not seem to differ qualitatively or quantitatively in the normal, BPH, or well-differentiated carcinoma acini. The most numerous class of cell is the microvillous cell. Variation in the number of microvilli from very sparse (2.5/100 sq. μ) to numerous, clumped microvilli covering the entire surface of the cell is striking, as is the variability in the length of the microvilli from short, stubby projections (0.1-0.2 μ length), to long finger-like projections (1-1.5 μ length).

There is great variation in the number and structure of projections which have been generally classified as "ruffles": short projections termed microplicae, or ridge-like, and more exaggerated structures which are actual ruffles. Ruffled cells have been identified in rat kidney collecting tubules (1, 5, 37), dog kidney collecting tubules (M. P. Stone, unpublished observations), the stratified squamous corneal epithelium of many species (2, 13, 15), and human lymphocytes and monocytes (17, 24, 25, 26). Some controversy has existed as to whether the ridge-like structures of human corneal epithelial cells are actually collapsed microvilli (22). The ruffles, or ridge-like structures, of the prostate apical cell membranes are clearly demonstrated by scanning electron stereomicrographs and transmission electron micrographs.

The bare cells mentioned previously are of two types, those with undulating membranes and those which appear as balloon-like structures. TEM sections (M. P. Stone, unpublished) suggest that the balloon-like structures are artifacts due to improper fixation. Transmission electron micrographs indicate that the smooth-surfaced balloon-like structure contains a very dispersed "watery" cytoplasm described previously (4). The bare cells with undulating membranes (Figs. 4, 5, and 6) demonstrate the general ultrastructure for prostate cells. The basal cytoplasm is generally compact. The round, or ovoid, nucleus is located in the basal portion of the cell, and the double membrane surrounding the nucleus is evident in most sections. Identifiable lipid droplets often appear in the perinuclear region. The Golgi apparatus and the endoplasmic reticulum are generally difficult to identify in those cells with numerous

secretory vacuoles. Convuluted cisternae of rough endoplasmic reticulum are present and mitochondria are scattered throughout the cytoplasm of the cell. Often the mitochondrial cristae are short and incomplete (as in Fig. 6) - a characteristic Mao et al. described for cuboidal acinar cells (20). The appearance of the mitochondria may be due to consecutive processing to SEM and TEM or to the lapse of time between excision and fixation of the tissue. Since the mitochondria of tissues processed only for TEM often have the same swollen appearance, the problem is probably one of poor fixation.

Though cell surface morphologies do not distinguish between normal, BPH, and well-differentiated adenocarcinomas there are limiting factors in this study. Proper fixation, as mentioned previously, is a problem. These samples are human tissues and, therefore, cannot be infused with fixative as is possible in animal model systems. The time of fixation after excision varied within an hour limit; this could have resulted in some distortion of acinar cell morphology. The criteria used to label acini as normal, BPH, and adenocarcinoma were size, shape, and the ordered arrangement of structural components. Though similar numbers of BPH (24) and adenocarcinoma (21) tissues were examined, significantly fewer acini could be identified as adenocarcinoma than BPH based on these criteria. The normal acini examined in this study were from adenocarcinoma tissues which had only discrete foci of adenocarcinoma. Attempts were made to obtain normal prostatic tissue at autopsy, but these samples generally proved unsuitable for SEM, either because of infection of the tissue, age of the patient, or time lapse before fixation of the tissue. The presence of prostatic secretion (as in Fig. 10b) could also have prejudiced the results. Several wash procedures were initiated to clear the acini of secretion but all proved detrimental to the surface structure of the scanned acinar cells; thus only those glands free of secretion during fixation could be examined for surface structure detail. These factors may have influenced the quantitative results of this study; however, all types of cell surface morphologies are present in normal, BPH, and adenocarcinoma acini. The three types of cell surface morphologies could be distinguished in a single scanning electron micrograph of a moderately-differentiated adenocarcinoma where the acinar cells were present in cords and sheets (35). This is rarely found; generally the acinar cells of poorly-differentiated adenocarcinomas present a different surface morphology than those described for the acinar

cells of normal, BPH, or well-differentiated adenocarcinomas. The cells of poorly-differentiated adenocarcinomas often appear in sheets rather than in acini and are devoid of surface structure. Critical point drying artifacts are more often seen in the poorly-differentiated adenocarcinomas than in the other tissues. The appearance of invasive prostatic acinar cells is similar to that found in mammary duct invasive carcinoma (32).

Though cell surface morphologies do not indicate the pathological state of the cell, cell surface morphology may provide information about the secretory state of the cell. The thin sections suggest a difference in the number of secretory granules and their content in cells with different surface morphologies. Acinar cells with elaborate microprojections often contain numerous secretory granules, many of them electron-dense. Acinar cells with short microvilli, or little surface structure, also contain secretory granules; however, these secretion granules are less numerous, less electron-dense, and not generally in close apposition to the apical membrane.

Both apocrine and merocrine secretion have been described for the human prostate (20). Apocrine secretion, in its original context, is the loss of the apical portion of the cells (3, 20) though this term has been used recently for the formation of blebs on the apical surface of the cell which eventually pinch off from the cell surface (41). Merocrine secretion involves the fusion of the secretion vacuole membrane with the cell apical membrane and the discharge of secretory materials into the acinar lumen. Combination SEM and TEM studies provide an important aid in viewing prostate secretion. The scanning electron micrographs illustrate several important variations in the form of secretions found in the acinar lumen. The fine granular material covering the cells in Figure 10b appear to illustrate merocrine secretion. Merocrine secretion is illustrated in the transmission electron micrographs Figure 5 and Figure 11c where small granules are extruded from the cell and are observed in the acinar lumen.

In Figure 10a a membrane enclosed bleb attached by a stalk-like projection to the cell surface may contain a secretory product. If so, it should eventually appear as a membrane-enclosed body in the acinar lumen. Numerous TEM sections appear to support this mechanism of secretion both in the prostate (3, 9, 20), and in mammary tissue (11, 16, 40, 41).

Figures 10c-e illustrate an interesting phenomenon - the appearance of "craters" in the surface of the cell with membrane-enclosed bodies in close apposition. There has been uncertainty concerning the origin of such

"craters". It has been argued that they are simply artifacts created by the collapse of apical vacuoles (15). However, the "craters" have a membrane "bottom" when photographed in stereo pairs. Holes in the cell membrane due to fixation and preparation artifacts have a different appearance; their outline is less smooth and there is no obvious membrane lining. The crater in Figure 10d could illustrate the phenomenon seen in Figure 11b where three secretion vacuoles have fused with the cell membrane and a fourth vacuole is nearing the cell surface. There is another secretory mechanism which would explain the craters and their relationship with the membrane enclosed bodies. Prostatic secretion contains lipid, much of it present in the form of globules (21, 23, 30). Studies of mammary tissue have shown that milk fat bodies are formed by apocrine secretion but there are indications that variations may occur in that process. Wooding (41) has described a process for the extrusion of milk fat bodies which would resemble Figures 10c and 10e (41). The milk fat body creates a bulge in the apical membrane and other vesicles fuse with the apical cell membrane causing invaginations. Clefts are formed beside the lipid body presenting a structure similar to the ruffles in Figure 10e and Figure 11c. The lipid body enclosed in cellular membrane is pinched off and the cell is left with a disrupted membrane in a crater-like depression which is quickly repaired. While this explanation is highly speculative it may represent a plausible mechanism for extrusion of lipid in the prostate and a plausible explanation for the relation of ruffles and both merocrine and apocrine secretion.

The final objective of this study is to attempt to correlate cell surface morphologies of prostatic acinar cells in tissue with cells cultured in vitro. It has been shown that the cells in tissue culture retain their surface morphology as they spread onto the surface of the petri dish (Fig. 3). At least a portion of the cells in culture are prostatic acinar cells, but there are no definitive surface morphological markers which prove that none of these cells are of endothelial origin. The great heterogeneity of cell surface morphology in well-differentiated adenocarcinoma, BPH, and normal tissues prevents a correlation of cell surface structure and tissue pathology. It also appears improbable that the surface morphology of a tissue culture cell can be used to correlate that cell with the pathology of the original acinar cell.

Acknowledgements. The authors acknowledge the helpful discussions and assistance of Dr. Sara Miller, Department of Microbiology, and

the helpful discussions of Dr. Juan Vergara, Department of Anatomy, and Dr. Craig Tisher, Department of Medicine, Duke University.

This work was supported by grant CA 15417 from the National Prostate Cancer Project and by the Medical Research Service of the Veterans Administration.

REFERENCES

1. Andrews, P. M., Porter, K. R.: A scanning electron microscopic study of the nephron. *American Journal of Anatomy* 140, 81 (1974)
2. Blumke, S., Morgenroth, K., Jr.: The stereo ultrastructure of the external and internal surface of the cornea. *Journal of Ultrastructure Research* 18, 502 (1967)
3. Brandes, D.: The fine structure and histochemistry of prostatic glands in relation to sex hormones. *International Review of Cytology* 20, 207 (1966)
4. Brandes, D., Kirchheim, D., Scott, W. W.: Ultrastructure of the human prostate: Normal and neoplastic. *Laboratory Investigation* 13, 1541 (1964)
5. Bulger, R. E., Siegel, F. L., Pendergrass, R.: Scanning and transmission electron microscopy of the rat kidney. *American Journal of Anatomy* 139, 483 (1974)
6. Chandra, S., Skelton, F. R.: Staining of juxtaglomerular cell granules with toluidine blue or with basic fuchsin for light microscopy after epon embedding. *Stain Technology* 39, 107 (1964)
7. Clark, M. A., O'Connell, K. J.: Scanning electron microscopic studies of normal and pathologic human genitourinary organs. A preliminary report. *Scanning Electron Microscopy/1973*, IIT Research Institute, Chicago, 581
8. Clark, M. A., O'Connell, K. J., Edson, M.: Scanning electron microscopic studies of control and hypertrophic human prostate glands. *Journal of Urology* 110, 558 (1973)
9. Fisher, E. R., Jeffrey, W.: Ultrastructure of human normal and neoplastic prostate. With comments relative to prostatic effects of hormonal stimulation in the rabbit. *American Journal of Clinical Pathology* 44, 119 (1965)
10. Fisher, E. R., Sieracki, J. C.: Ultrastructure of human normal and neoplastic prostate. *Pathologic Annual* 5, 1 (1970)
11. Franke, W. W., Luder, M. R., Kartenbeck, J., Zerban, H., Keenan, T. W.: Involvement of vesicle coat material in casein secretion and surface regeneration. *Journal of Cell Biology* 69, 173 (1976)
12. Golomb, H. M., Reese, C.: Surface ultrastructural and marker characteristics of leukemic cells. *Scanning Electron Microscopy/1976/II*, IIT Research Institute, Chicago, 42
13. Harding, C. V., Bagchi, M., Weinsieder, A., Peters, V.: A comparative study of corneal epithelial cell surfaces utilizing the scanning electron microscope. *Investigative Ophthalmology* 13, 906 (1974)
14. Hauschka, S. D., Konigsberg, I. R.: The influence of collagen on the development of muscle clones. *Proceedings of the National Academy of Sciences* 55, 119 (1966)
15. Hoffman, F., Schweichel, J. U.: The microvilli structure of the corneal epithelium of the rabbit in relation to cell function. *Ophthalmologic Research* 4, 175 (1972/73)
16. Kurosumi, K.: Electron microscopic analysis of the secretion mechanism. *International Review of Cytology* XI, 1 (1961)
17. Lin, P. S., Cooper, A. G., Wortis, H. H.: Scanning electron microscopy of human T cell and B cell rosettes. *New England Journal of Medicine* 289, 548 (1973)
18. Luft, J. H.: Improvements in epoxy resin embedding methods. *Journal of Biophysical and Biochemical Cytology* 9, 409 (1961)
19. Mao, P., Nakao, K., Angrist, A.: Human prostatic carcinoma: An electron microscope study. *Cancer Research* 26, 955 (1966)
20. Mao, P., Nakao, K., Bora, R., Geller, J.: Human benign prostatic hyperplasia. *Archives of Pathology* 79, 270 (1965)
21. Nylander, G.: The electrophoretic pattern of prostatic lipid secretion in normal and pathological conditions. *Scandinavian Journal of Clinical and Laboratory Investigation* 7, 250 (1955)
22. Pfister, R. R.: The normal surface of corneal epithelium: a scanning electron microscopic study. *Investigative Ophthalmology* 12, 654 (1973)
23. Plenge, Carl: Ulser lipoide und pigmente der prostata des menschen. *Virchow's Archiv Pathologische Anatomie* 253, 665 (1924)
24. Polliack, A.: Surface features of circulating human leukemic cells: Experience with 175 cases of leukemia examined by scanning electron microscopy. *Scanning Electron Microscopy/1976/II*, IIT Research Institute, Chicago, 33
25. Polliack, A., Lampen, N., Clarkson, B. D., de Harven, E., Bertwich, A., Siegal, F. P., Kunkel, H. G.: Identification of human B and T lymphocytes by scanning

- electron microscopy. *Journal of Experimental Medicine* 138, 607 (1973)
26. Polliack, A., Lampen, N., de Harven, E.: Scanning electron microscopy of lymphocytes of known B and T derivation. *Scanning Electron Microscopy/1974*, IIT Research Institute, Chicago, 673
 27. Richardson, K.C., Jarrett, L., Finke, E.H.: Embedding in epoxy resins for ultrathin sectioning in electron microscopy. *Stain Technology* 35, 313 (1960)
 28. Riddell, R.J., Eisenstat, L., Levin, B., Golomb, H.: Surface ultrastructure of human adenomatous and hyperplastic polyps. *Scanning Electron Microscopy/1976/II*, IIT Research Institute, Chicago, 19
 29. Sato, T.: A modified method for lead staining of thin sections. *Journal of Electronmicroscopy* 16, 133 (1967)
 30. Scott, W.W.: The lipids of the prostatic fluid, seminal plasma, and enlarged prostate gland of man. *Journal of Urology* 53, 712 (1945)
 31. Siew, S.: Scanning electron microscopy of neoplastic lesions of the human colon. *Scanning Electron Microscopy/1976/II*, IIT Research Institute, Chicago, 11
 32. Spring-Mills, E., and Elias, J.J.: Cell surface changes associated with human breast cancer. *Scanning Electron Microscopy/1976/II*, IIT Research Institute Chicago, 1
 33. Spurlock, B.O., Skinner, M.S., Kattine, A.A.: A simple rapid method for staining epoxy-embedded specimens for light microscopy with the polychromatic stain paragon - 1301. *American Journal of Clinical Pathology* 46, 252 (1966)
 34. Stone, K.R., Stone, M.P., Paulson, D.F.: In vitro cultivation of prostatic epithelium. *Investigative Urology* 14, 79 (1976)
 35. Stone, M.P., Stone, K.R., Paulson, D.F.: Scanning electron microscopy of hyperplastic and neoplastic human prostate. *Urological Research* 4, 71 (1976)
 36. Takayasu, H., and Yamaguchi, Y.: An electron microscopic study of the prostatic cancer cell. *Journal of Urology* 87, 935 (1962)
 37. Tisher, C.: personal communication
 38. Watson, M.L.: Staining of tissue sections for electron microscopy with heavy metals. *Journal of Biophysical and Biochemical Cytology* 4, 475 (1958)
 39. Westbrook, E., Wetzel, B., Cannon, G.B., Berard, D.: The impact of culture conditions on the surface morphology of cells in vitro. *Scanning Electron. Microscopy/1975*, IIT Research Institute, Chicago, 352
 40. Wooding, F.B.P.: The mechanism of secretion of the milk fat globule. *Journal of Cell Science* 9, 805 (1971)
 41. Wooding, F.B.P.: Formation of the milk fat globule membrane without participation of the plasmalemma. *Journal of Cell Science* 13, 221 (1973)

Dr. David F. Paulson
 Department of Surgery
 Division of Urology
 Duke University Medical Center
 Durham, NC 27710
 USA